Spin Fluctuations in the 0.7 Anomaly in Quantum Point Contacts

Dennis H. Schimmel,[1] Benedikt Bruognolo,[1,2] and Jan von Delft[1]
[1]Physics Department, Arnold Sommerfeld Center for Theoretical Physics, and Center for NanoScience, Ludwig-Maximilians-Universität, Theresienstraße 37, 80333 Munich, Germany
[2]Max-Planck-Institut für Quantenoptik, Hans-Kopfermann-Straße 1, 85748 Garching, Germany
(Received 9 March 2017; revised manuscript received 1 June 2017; published 7 November 2017)

It has been argued that the 0.7 anomaly in quantum point contacts (QPCs) is due to an enhanced density of states at the top of the QPC barrier (the van Hove ridge), which strongly enhances the effects of interactions. Here, we analyze their effect on dynamical quantities. We find that they pin the van Hove ridge to the chemical potential when the QPC is subopen, cause a temperature dependence for the linear conductance that qualitatively agrees with experiments, strongly enhance the magnitude of the dynamical spin susceptibility, and significantly lengthen the QPC traversal time. We conclude that electrons traverse the QPC via a slowly fluctuating spin structure of finite spatial extent.

DOI: 10.1103/PhysRevLett.119.196401

Quantum point contacts are narrow, one-dimensional (1D) constrictions usually patterned in a two-dimensional electron system by applying voltages to local gates. As quantum point contacts (QPCs) are the ultimate building blocks for controlling nanoscale electron transport, much effort has been devoted to understanding their behavior at a fundamental level. Nevertheless, in spite of a quarter of a century of intensive research into the subject, some aspects of their behavior still remain puzzling.

When a QPC is opened up by sweeping the gate voltage, V_g, that controls its width, its linear conductance famously rises in integer steps of the conductance quantum, $G_Q = 2e^2/h$ [1,2]. This conductance quantization is well understood [3] and constitutes one of the foundations of mesoscopic physics. However, during the first conductance step, where the dimensionless conductance $g = G/G_Q$ changes from 0 to 1 (from a "closed" to an "open" QPC), an unexpected shoulder is generically observed near $g \simeq 0.7$. More generally, the conductance shows anomalous behavior as a function of temperature (T), magnetic field (B), and source-drain voltage (V_{sd}) throughout the regime $0.5 \lesssim g \lesssim 0.9$, where the QPC is "subopen." The source of this behavior, collectively known as the "0.7 anomaly," has been controversially discussed [4–23] ever since it was first systematically described in 1996 [4]. Though no consensus has yet been reached regarding its detailed microscopic origin [10,22], general agreement exists that it involves electron spin dynamics and geometrically enhanced interaction effects.

In this Letter, we further explore the van Hove ridge scenario proposed in Ref. [22]. It asserts that the 0.7 anomaly is a direct consequence of a "van Hove ridge," i.e., a smeared van Hove peak in the energy-resolved local density of states (LDOS) $\mathcal{A}_i(\omega)$ at the bottom of the lowest 1D subband of the QPC. Its shape follows that of the QPC barrier [22–24] and, in the subopen regime, where the barrier top lies just below the chemical potential μ, it causes the LDOS *at* μ to be strongly enhanced. This reflects the fact that electrons slow down while crossing the QPC barrier [since the semiclassical velocity of an electron with energy ω at position i is inversely proportional to the LDOS, $\mathcal{A}_i(\omega) \sim v^{-1}$]. The slow electrons experience strongly enhanced mutual interactions, with striking consequences for various physical properties.

In this Letter, we elucidate their effect on various *dynamical* quantities, which govern those aspects of the 0.7 anomaly that probe finite-energy excitations. To this end, we compute real-frequency correlation functions computed using the functional renormalization group (FRG) on the Keldysh contour [25–28]. We compute (i) the energy dependence of the LDOS, finding that its maximum is pinned to μ in the subopen regime due to a Hartree increase in the barrier height with increasing density, (ii) the temperature dependence of the linear conductance, finding qualitative agreement with experiments, (iii) the dynamical spin susceptibility $\chi(\omega)$, from which we extract a characteristic time scale t_{spin} for spin fluctuations, and (iv) the time t_{trav} for a quasiparticle to traverse the QPC, which we extract from the single-particle scattering matrix $S(\omega)$. Intermediate interaction strengths suffice to obtain the characteristic 0.7 shoulder at finite temperatures. We find strong links among the ω dependence of the spin susceptibility, the one-particle S matrix, and the form of the LDOS. As long as the van Hove ridge is pinned to μ, interactions cause relevant degrees of freedom to slow down, inducing significant increases in both t_{trav} and t_{spin}. Moreover, these two times are comparable in magnitude, implying that a quasiparticle traversing the QPC encounters a quasistatic spin background. This provides links to other proposed explanations of the 0.7 anomaly [4–18].

Model.—Focusing on the first subband, we model the QPC by a smooth potential barrier describing the effective

1D potential along the transport direction. After discretizing the longitudinal position coordinate as $x = ai$, with site index i and lattice spacing a, the model Hamiltonian has the form [22]

$$\mathcal{H} = -\sum_{\sigma,i} \tau_i (c^\dagger_{i+1,\sigma} c_{i,\sigma} + \text{H.c.}) + \sum_i U_i c^\dagger_{i\uparrow} c_{i\uparrow} c^\dagger_{i\downarrow} c_{i\downarrow}. \quad (1)$$

It describes an infinite tight-binding chain with nearest-neighbor hopping τ_i of quasiparticles with spin $\sigma = \uparrow, \downarrow$ and short-range interactions U_i. The hopping amplitude τ_i varies smoothly with i, thus creating an effective potential barrier $V_i = -(\tau_i + \tau_{i+1}) + 2\tau$ measured with respect to the leads' band bottom -2τ. We choose $U_i \neq 0$ and $\tau_i \neq \tau$ for $N = 2N' + 1$ sites only, symmetric around $i = 0$, that define the extent of the QPC (central region). U_i is constant in the center of the QPC with $U_0 = U$ and drops smoothly to zero as i approaches the edges of the central region at sites $\pm N'$. We tune the hopping such that the effective barrier is symmetric and parabolic near the top, $V_i = \tilde{V}_c - i^2\Omega_x^2/(2\tau)$, where the barrier height $\tilde{V}_c$ mimics the role of gate voltage from an experiment, and the curvature Ω_x sets the characteristic length scale $l_x = a\sqrt{\tau/\Omega_x}$ of the QPC. We sweep $\tilde{V}_c$ such that the barrier crosses the chemical potential μ. The precise form of U_i and τ_i is given in Sec. S-I of the Supplemental Material [29]. The model is solved with the perturbatively truncated Keldysh FRG in equilibrium (see Sec. S-II of the Supplemental Material [29]). We use $\tau = 1$, $U = 0.7\tau$, $\mu = -1.475\tau$, $V_c = \tilde{V}_c - \mu - 2\tau \in [-2.83, 1.83]\Omega_x$, and $\Omega_x \approx 0.03\tau$ (with $\hbar = 1$).

Local density of states.—It was argued in Ref. [22] that the physics of the QPC is governed by the LDOS, $\mathcal{A}_i(\omega) = -(1/\pi)\text{Im}G^R_{ii}(\omega)$, where G^R_{ij} is the retarded single-particle Green's function between sites i and j. Figures 1(a)–1(c) show the bare LDOS $\mathcal{A}_i^{U=0}(\omega)$ of the QPC as a function of site i and energy ω at three values of the barrier height V_c. The bare LDOS has a maximum just above the band bottom, visible as a red structure, that follows the shape of the effective potential (the thick white line). This structure is the bare van Hove ridge discussed in Ref. [22], the apex of which has a maximum value $\sim(\Omega_x\tau)^{-1/2}$, and occurs at an energy $\omega_{\max}(V_c)$ that lies slightly higher than the bare potential maximum V_0, by an amount $\sim\Omega_x$.

Upon adding interactions, we obtain Figs. 1(d)–1(f), which shows two striking differences to the noninteracting case: In the (sub)open regime, the renormalized van Hove ridge is shifted upward in energy ($\omega_{\max}$ is larger) and becomes flatter spatially. Both of these effects may *qualitatively* be understood by a mean field argument [37,38]: The slope of the van Hove ridge may be interpreted as reflecting the shape of an effective, renormalized potential barrier, which is shifted upward relative to the bare barrier

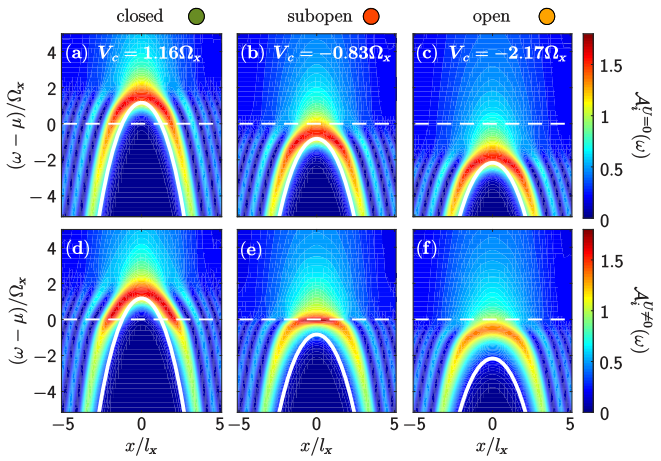

FIG. 1. van Hove ridge in the LDOS $\mathcal{A}_i(\omega)$ (color scale) of (a,b,c) a noninteracting and (d,e,f) an interacting QPC, plotted as a function of energy $\omega - \mu$ and position $x = ai$. The thick solid white line depicts the effective bare potential barrier V_i, the thin dashed white line, and the chemical potential μ. Closed (a,d), subopen (b,e), and open (c,f) regimes are shown from left to right. With interactions, the van Hove ridge is shifted upward and flattened in the (sub)open regime [compare (b) and (e) to (c) and (f)].

by a Hartree shift proportional to the local electron density. Away from the center, the density is higher, such that the shift is larger, causing the van Hove ridge to become flatter as a function of x near its apex, while becoming narrower and higher as a function of ω. This is also seen clearly in Fig. 2(a), which shows the interacting (solid lines) and bare (dashed lines) LDOS $\mathcal{A}_0(\omega)$. The x flattening and ω sharpening is most striking in the subopen regime, where the van Hove ridge apex intersects the chemical potential [Fig. 1(e)], because the interaction-induced effects are largest there. We have checked our Keldysh-FRG results against density matrix renormalization group (DMRG) computations of the system with somewhat different parameters, finding good qualitative agreement and, specifically, the same values for $\omega_{\max}$ (see Sec. S-III of the Supplemental Material [29]).

The evolution of $\mathcal{A}_0(\omega)$ as V_c is varied is shown in Fig. 2(c). As V_c is lowered, the energy $\omega_{\max}$ of the van Hove ridge maximum follows the bare barrier top (the solid white line) as long as the QPC is closed, then remains *pinned* at the chemical potential throughout the subopen regime to form a plateaulike structure, and finally decreases again only deep in the open regime [compare this to Fig. 1(d) of Ref. [37]]. The plateaulike structure sets in once the bare barrier top V_0 drops below the chemical potential because then the electron density near the QPC center begins to increase, leading to an upward Hartree shift of the barrier height that almost compensates for the decrease in V_c [37]. This pinning is the reason why the conductance step at zero temperature is asymmetric [compared to the noninteracting case, the dashed line in Fig. 2(d)],

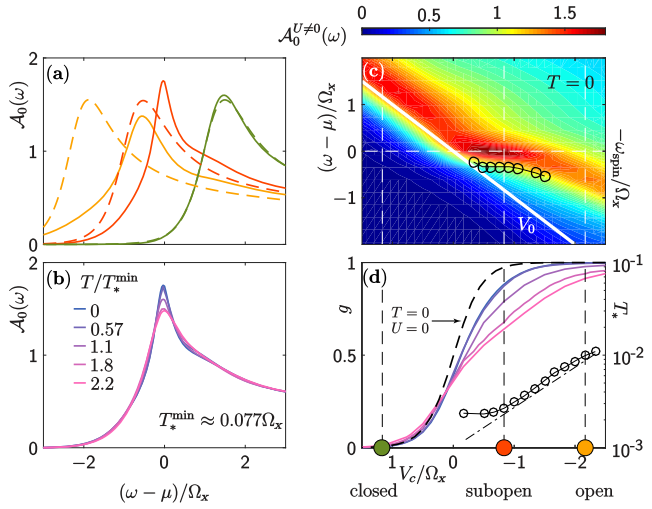

FIG. 2. (a) The interacting LDOS (the solid lines) and bare LDOS (the dashed lines), plotted as a function of energy ω for three values of V_c, indicated by dots of corresponding color in (c), (d). In the subopen (red) and open (orange) regimes, interactions shift the van Hove peak to larger energies, as the barrier height is renormalized. Moreover, in the subopen regime, flattening of the van Hove ridge causes the peak to become sharper and higher. (b) $\mathcal{A}_0(\omega)$ in the subopen regime for several different temperatures. At larger temperatures, the maximum is lower as weight is shifted into the flanks of the van Hove ridge and redistributed in the band. (c) $\mathcal{A}_0(\omega)$, the interacting LDOS (color scale) at the central site, as a function of ω and V_c. The solid white line shows the bare barrier height, V_0. In the subopen regime, the energy of the van Hove ridge maximum, $\omega_{\max}$, is pinned to the chemical potential. The black circles show the characteristic energy $\omega_{\rm spin}$ of the spin susceptibility χ. They clearly follow the LDOS maximum. (d) Conductance g (left axis) for different temperatures (the dashed curve, g for $T=U=0$), and T_* (the circles), extracted via Eq. (2), shown on a logarithmic scale (right axis). Temperature is measured in units of $T_*^{\min}=\min T_*(V_c)$. As a guide for the eye, $0.001\exp(-V_c/\Omega_x)$ (the dashed-dotted line). Our FRG results qualitatively reproduce the generic feature common to numerous experiments [29], namely, a strong reduction of g with increasing T in the subopen regime, causing an increasing asymmetry in the conductance step.

changing much more slowly with V_c for $g \gtrsim 0.5$ than for $g \lesssim 0.5$.

Finite temperature.—This structure sheds new light on the temperature dependence of the linear conductance on temperature. When the temperature, T, is increased, the van Hove peak in the LDOS retains its overall shape and is broadened only slightly (for $T \lesssim \Omega_x/10$) [Fig. 2(b)]. At the same time, the first conductance step is flattened out in a characteristic, asymmetric fashion [Fig. 2(d)], in qualitative agreement with experiments (see Sec. S-IV of the Supplemental Material [29]). This can be understood as follows [22]: Increasing T increases the available phase space for inelastic scattering, thus enhancing interaction effects. Their strength is governed by the LDOS near the chemical potential, which is particularly large *throughout the subopen region* due to the pinning of $\omega_{\max}$ to the chemical potential. Accordingly, interaction-induced backscattering is large in the whole subopen regime, leading to a strong suppression of the conductance [Fig. 2(d)] even into the open regime. At pinch-off, the conductance is slightly increased due to thermal activation.

To quantify the strength of the temperature dependence as a function of V_c, we expand the conductance as

$$g(T,V_c) = g(0,V_c) - T^2/T_*^2(V_c) + \mathcal{O}(T^3), \qquad (2)$$

as appropriate for a Fermi liquid [22]. The $T_*(V_c)$ values extracted from our finite-T data [see Fig. 2(d), the circles] depend roughly exponentially on gate voltage $T_*(V_c) \sim \exp(-V_c/\Omega_x)$ [Fig. 2(d), the dashed-dotted line], when the QPC is tuned from subopen to open, reflecting the V_c dependence of the bare QPC transmission rate [22].

Spin susceptibility.—In the van Hove ridge scenario, a key property of a subopen QPC is the presence of "slow spin fluctuations" [22], as advocated for also in Ref. [39]. To explore this, we have computed the dynamical equilibrium spin susceptibility,

$$\chi_{ij}(\omega) = \int dt \langle \mathcal{T} S_i^z(t) S_j^z(0)\rangle \exp(i\omega t), \qquad (3)$$

where $\mathcal{T}$ denotes time ordering. In a Fermi liquid, the spin susceptibility is determined by the particle-hole bubble and thus governed by single-particle properties. However, due to the inhomogeneity of the QPC, both the energy and the position dependence of the spin susceptibility are nontrivial. For now, we focus on χ_{0j}, shown in Fig. 3, which has the following salient features.

(i) χ_{0j} oscillates with a spatially varying wavelength which becomes shorter as the QPC is opened or the energy is increased. For small energies ω, the wavelength of these oscillations is determined by the "local Fermi wavelength" λ_F, which can be extracted from $|\mathrm{Im}G_{0j}^R(\mu)|$ (the blue line in Fig. 3). In the subopen regime, λ_F is large in the center, where the density is small, such that the sign of the spin susceptibility changes only far away from the center. Thus, an excited spin in the center leads to a rather large cloud (covering a region of $\sim 3l_x$) of co-oriented spins. Away from the QPC, the oscillations in χ_{0j} simply follow the Friedel oscillations.

(ii) On the central site, $\chi_{00}(\omega)$ shows a clear characteristic at an energy $\omega_{\rm spin}(V_c)$, whose dependence on V_c follows that of $\omega_{\max}$ [$-\omega_{\rm spin}$ is indicated by black circles in Fig. 2(c)]. In general, for small energies, $\omega_{\rm spin}$ is set by the distance between the chemical potential and the nearest peak in the LDOS (see Sec. S-V of the Supplemental Material [29]).

(iii) The spin susceptibility $\chi_{0i}(\omega)$ is amplified by interactions (Stoner physics) [compare Figs. 3(a)–3(c) to Figs. 3(d)–3(f), and also Fig. 4(a) to Fig. 4(b)]. Interactions

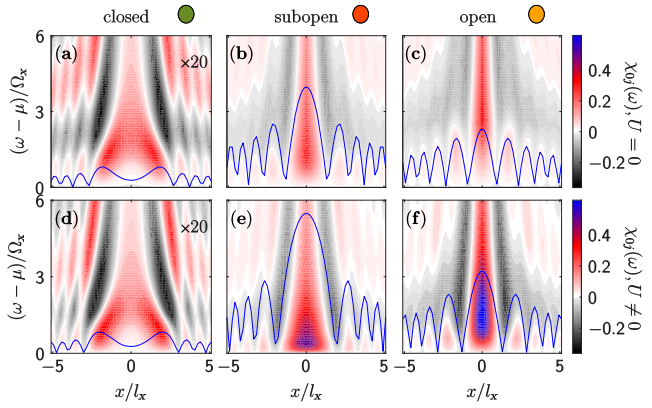

FIG. 3. (a)–(c) Noninteracting and (d)–(f) interacting dynamical spin susceptibility [multiplied by a factor of 20 in order to be visible in (a) and (d)] for a closed, a subopen, and an open QPC. The blue line shows $|\mathrm{Im}[G_{0i}(\omega=\mu)]|$ (arbitrary units).

also amplify the temperature-induced reduction of the spin susceptibility at ω_{spin} [Figs. 4(a) and 4(b)]. This effect is of a similar strength as the decrease of the LDOS at ω_{max} [Fig. 2(b)].

Traversal time.—The traversal time t_{trav} for a single incident quasiparticle with energy ω to traverse a scattering region can be obtained by a procedure attributed to Wigner [40], which relates it to the scattering-induced dispersion of the incident wave packet: It is given by

$$t_{\mathrm{trav}}(\omega)=t_0(\omega)+t_{\mathrm{delay}}(\omega), \quad t_{\mathrm{delay}}(\omega)=2\partial_\omega\phi(\omega), \quad (4)$$

where $t_0(\omega)$ is the traversal time through the central region with the potential and interactions being turned off, t_{delay} and $\phi(\omega)$ are the delay time and the scattering phase shift due to the potential- and interaction-induced slowdown of the quasiparticles. In our setup, $\phi(\omega)$ is the phase of the left-right component of the zero-temperature single-particle S matrix,

$$S_{l,r}(\omega) = -2\pi i\tau\rho(\omega)G^R_{-N',N'}(\omega), \quad (5)$$

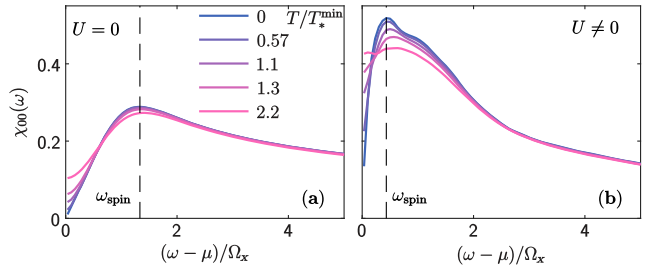

FIG. 4. (a) Noninteracting and (b) interacting spin-spin correlations on the central site in the subopen regime at different temperatures; i.e., the blue lines are vertical cuts of Figs. 3(b) and 3(e) through $x=0$. The dashed black line is at $\omega=\omega_{\mathrm{spin}}$. The shoulder in (b) is due to the LDOS-dependent enhancement of the spin susceptibility due to interactions.

where $\rho(\omega)$ is the lead density of states at the sites $\pm(N'+1)$ in the absence of the central region and τ is the hopping amplitude there. $|S_{l,r}(\omega)|^2$ yields the transmission probability. Figures 5(a) and 5(b) show the traversal time. Though calculated from a nonlocal correlation function, its behavior is strikingly similar to that of the LDOS at the central site, Fig. 2(c). This is consistent with the semiclassical interpretation $\mathcal{A}\sim v^{-1}$: Whenever the LDOS is large, quasiparticles are slow, and thus a large time is required to traverse the QPC.

Interestingly, we find that in the subopen regime the traversal time t_{trav} is of the same order as the characteristic time scale, $t_{\mathrm{spin}}=(2\pi/\omega_{\mathrm{spin}})$, associated with spin fluctuations, namely, $t_{\mathrm{trav}}\lesssim 8/\Omega_x$ and $t_{\mathrm{spin}}\lesssim 10/\Omega_x$. We note that, with our parameters, $t_0\approx 1.3/\Omega_x$; thus, t_{trav} is dominated by the delay time. That t_{trav} and t_{spin} are comparable in magnitude is consistent with a Fermi-liquid description of the system (which underlies the FRG method used here): The only stable degrees of freedom in a Fermi liquid are dressed electron- and holelike quasiparticles, and spin fluctuations arise via electron-hole–like excitations. Near the QPC center ($x\lesssim l_x$), the lifetime of spin fluctuations is thus governed by the quasiparticle decay time. Heuristically, this roughly corresponds to t_{trav}, as the region where interaction effects are strongest extends over only a few λ_F oscillations. Though we find no static contributions to the dynamical spin susceptibility at zero magnetic field, the fact that $t_{\mathrm{spin}}\simeq t_{\mathrm{trav}}$, together with the extended spatial structure of the spin susceptibility in the subopen regime, suggests the heuristic view that a quasiparticle traversing the QPC encounters a quasistatic, spatially coherent spin environment.

Discussion.—Our results allow us to establish contact with two other prominent scenarios that have been proposed to explain the 0.7 anomaly. (i) According to the

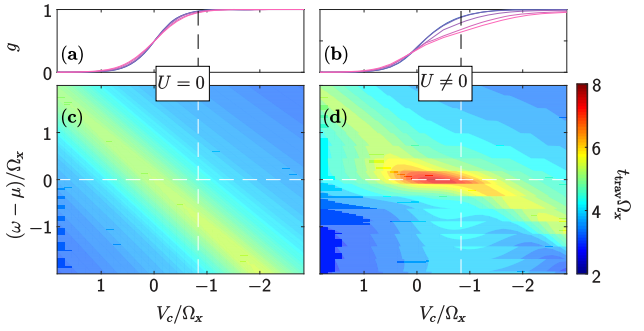

FIG. 5. Comparison of (a), (c) noninteracting and (b), (d) interacting traversal time. (a), (b) Conductance g, as a function of gate voltage V_c, to identify the closed, subopen, and open regimes. The color code is identical to Fig. 2. (c), (d) Traversal time [Eq. (4)] as a function of energy ω and gate voltage V_c. While the traversal time of modes below the barrier is small, these modes have a low transmission probability and are irrelevant when determining the time scale of transport.

"spin-polarization scenario," interactions cause the spin degree of freedom in the QPC to spontaneously polarize, giving rise to a nonzero magnetization even at vanishing magnetic field, $B = 0$ [4–9,14–18]. (ii) According to the "quasilocalized spin scenario" proposed by Meir *et al.* [13], a subopen QPC hosts a quasilocalized state involving a spin-1/2 magnetic moment, causing Kondo-like conductance anomalies [10–13]. At low energies, a quasilocalized spin would be screened, giving rise to Fermi-liquid behavior that includes slow spin fluctuations. These two scenarios thus seem to offer starkly contrasting views of the spin structure in a QPC: (i) spatially extended but static in time vs (ii) spatially localized but fluctuating in time. Our work suggests that a view that entails elements of both: The spin structure fluctuates in time, in accord with (ii), but *slowly*—which is compatible with (i) if one is willing to reinterpret "spontaneous polarization" as "slowly fluctuating polarization." Also, the spin structure is spatially coherent, in accord with (i), over a region of *finite extent*—which is compatible with (ii) if one is willing to associate a nonzero spatial extent and a finite lifetime with the quasilocalized state evoked there. We thus suggest that the controversy between the opposing views (i) and (ii) can be resolved by associating the quasilocalized state evoked in (ii) with the slow electrons of the van Hove ridge, and by realizing that these constitute a quasistatic, spatially coherent spin environment, in the spirit of (i), for electrons traversing the QPC. Thus, though the various scenarios differ substantially in their details (and if one insists on comparing these details, the controversy will never be put to rest), they can be argued to have a common core: a slowly fluctuating spin structure of finite spatial extent in the center of the QPC. Moreover, our work shows that this spin structure originates naturally from the same interplay of interactions and QPC barrier geometry, encoded in the van Hove ridge, that causes transport properties to be anomalous.

We thank F. Bauer, J. Heyder, Y. Meir, S. Ludwig, and L. Weidinger for the useful discussions. B. B. thanks S. R. White for the discussions on the DMRG setup. The authors acknowledge support from the Deutsche Forschungsgemeinschaft (DFG) through the Excellence Cluster "Nanosystems Initiative Munich."

[1] D. A. Wharam, T. J. Thornton, R. Newbury, M. Pepper, H. Ahmed, J. E. F. Frost, D. G. Hasko, D. C. Peacock, D. A. Ritchie, and G. A. C. Jones, J. Phys. C **21**, L209 (1988).
[2] B. J. van Wees, H. van Houten, C. W. J. Beenakker, J. G. Williamson, L. P. Kouwenhoven, D. van der Marel, and C. T. Foxon, Phys. Rev. Lett. **60**, 848 (1988).
[3] M. Büttiker, Phys. Rev. B **41**, 7906 (1990).
[4] K. J. Thomas, J. T. Nicholls, M. Y. Simmons, M. Pepper, D. R. Mace, and D. A. Ritchie, Phys. Rev. Lett. **77**, 135 (1996); K. J. Thomas, J. T. Nicholls, N. J. Appleyard, M. Y. Simmons, M. Pepper, D. R. Mace, W. R. Tribe, and D. A. Ritchie, Phys. Rev. B **58**, 4846 (1998).
[5] D. J. Reilly, T. M. Buehler, J. L. O'Brien, A. R. Hamilton, A. S. Dzurak, R. G. Clark, B. E. Kane, L. N. Pfeiffer, and K. W. West, Phys. Rev. Lett. **89**, 246801 (2002).
[6] D. J. Reilly, Phys. Rev. B **72**, 033309 (2005).
[7] P. Jaksch, I. Yakimenko, and K.-F. Berggren, Phys. Rev. B **74**, 235320 (2006).
[8] E. Koop, A. Lerescu, J. Liu, B. van Wees, D. Reuter, A. D. Wieck, and C. van der Wal, J. Supercond. Novel Magn. **20**, 433 (2007).
[9] L. W. Smith, A. R. Hamilton, K. J. Thomas, M. Pepper, I. Farrer, J. P. Griffiths, G. A. C. Jones, and D. A. Ritchie, Phys. Rev. Lett. **107**, 126801 (2011).
[10] M. J. Iqbal, R. Levy, E. J. Koop, J. B. Dekker, J. P. de Jong, J. H. M. van der Velde, D. Reuter, A. D. Wieck, R. Aguado, Y. Meir, and C. H. van der Wal, Nature (London) **501**, 79 (2013).
[11] B. Brun, F. Martins, S. Faniel, B. Hackens, G. Bachelier, A. Cavanna, C. Ulysse, A. Ouerghi, U. Gennser, D. Mailly, S. Huant, V. Bayot, M. Sanquer, and H. Sellier, Nat. Commun. **5**, 4290 (2014).
[12] S. M. Cronenwett, H. J. Lynch, D. Goldhaber-Gordon, L. P. Kouwenhoven, C. M. Marcus, K. Hirose, N. S. Wingreen, and V. Umansky, Phys. Rev. Lett. **88**, 226805 (2002).
[13] Y. Meir, K. Hirose, and N. S. Wingreen, Phys. Rev. Lett. **89**, 196802 (2002); K. Hirose, Y. Meir, and N. S. Wingreen, Phys. Rev. Lett. **90**, 026804 (2003); A. Golub, T. Aono, and Y. Meir, Phys. Rev. Lett. **97**, 186801 (2006); T. Rejec and Y. Meir, Nature (London) **442**, 900 (2006).
[14] T.-M. Chen, A. C. Graham, M. Pepper, I. Farrer, and D. A. Ritchie, Appl. Phys. Lett. **93**, 032102 (2008).
[15] T.-M. Chen, A. C. Graham, M. Pepper, I. Farrer, D. Anderson, G. A. C. Jones, and D. A. Ritchie, Nano Lett. **10**, 2330 (2010).
[16] T.-M. Chen, M. Pepper, I. Farrer, G. A. C. Jones, and D. A. Ritchie, Phys. Rev. Lett. **109**, 177202 (2012).
[17] R. M. Potok, J. A. Folk, C. M. Marcus, and V. Umansky, Phys. Rev. Lett. **89**, 266602 (2002).
[18] C.-K. Wang and K.-F. Berggren, Phys. Rev. B **54**, R14257 (1996); **57**, 4552 (1998).
[19] A. P. Micolich, J. Phys. Condens. Matter **23**, 443201 (2011).
[20] Y. Komijani, M. Csontos, I. Shorubalko, T. Ihn, K. Ensslin, Y. Meir, D. Reuter, and A. D. Wieck, Europhys. Lett. **91**, 67010 (2010).
[21] Y. Chung, S. Jo, D.-I. Chang, H.-J. Lee, M. Zaffalon, V. Umansky, and M. Heiblum, Phys. Rev. B **76**, 035316 (2007).
[22] F. Bauer, J. Heyder, E. Schubert, D. Borowsky, D. Taubert, B. Bruognolo, D. Schuh, W. Wegscheider, J. von Delft, and S. Ludwig, Nature (London) **501**, 73 (2013).
[23] J. Heyder, F. Bauer, D. Schimmel, and J. von Delft, Phys. Rev. B **96**, 125141 (2017).
[24] F. Bauer, J. Heyder, and J. von Delft, Phys. Rev. B **89**, 045128 (2014); J. Heyder, F. Bauer, E. Schubert, D. Borowsky, D. Schuh, W. Wegscheider, J. von Delft, and S. Ludwig, Phys. Rev. B **92**, 195401 (2015).
[25] S. G. Jakobs, M. Pletyukhov, and H. Schoeller, Phys. Rev. B **81**, 195109 (2010).
[26] S. G. Jakobs, M. Pletyukhov, and H. Schoeller, J. Phys. A **43**, 103001 (2010).

[27] C. Karrasch, T. Enss, and V. Meden, Phys. Rev. B **73**, 235337 (2006).
[28] W. Metzner, M. Salmhofer, C. Honerkamp, V. Meden, and K. Schönhammer, Rev. Mod. Phys. **84**, 299 (2012).
[29] See Supplemental Material at http://link.aps.org/supplemental/10.1103/PhysRevLett.119.196401, which includes Refs. [30–36], for technical details pertaining to our calculations.
[30] U. Schollwöck, Rev. Mod. Phys. **77**, 259 (2005); Ann. Phys. (Amsterdam) **326**, 96 (2011); S. R. White, Phys. Rev. Lett. **69**, 2863 (1992); Phys. Rev. B **48**, 10345 (1993).
[31] M. Vekić and S. R. White, Phys. Rev. B **53**, 14552 (1996); Phys. Rev. Lett. **71**, 4283 (1993).
[32] G. Vidal, Phys. Rev. Lett. **93**, 040502 (2004); A. J. Daley, C. Kollath, U. Schollwöck, and G. Vidal, J. Stat. Mech. (2004) P04005; S. R. White and A. E. Feiguin, Phys. Rev. Lett. **93**, 076401 (2004).
[33] S. R. White and I. Affleck, Phys. Rev. B **77**, 134437 (2008); T. Barthel, U. Schollwöck, and S. R. White, Phys. Rev. B **79**, 245101 (2009).
[34] A. Weichselbaum, Ann. Phys. (Amsterdam) **327**, 2972 (2012).
[35] A. Kristensen, H. Bruus, A. E. Hansen, J. B. Jensen, P. E. Lindelof, C. J. Marckmann, J. Nygård, C. B. Sørensen, F. Beuscher, A. Forchel, and M. Michel, Phys. Rev. B **62**, 10950 (2000).
[36] F. B. Kugler and J. von Delft, arXiv:1703.06505; arXiv:1707.04536.
[37] S. Ihnatsenka and I. V. Zozoulenko, Phys. Rev. B **79**, 235313 (2009).
[38] A. X. Sánchez and J.-P. Leburton, Phys. Rev. B **88**, 075305 (2013).
[39] K. Aryanpour and J. E. Han, Phys. Rev. Lett. **102**, 056805 (2009).
[40] E. P. Wigner, Phys. Rev. **98**, 145 (1955).